Raman spectroscopy study of anodic film on $Ag_{43}Cu_{37}Zn_{20}$ alloy

S. P. DIMITRIJEVIĆ[a], Z. Ž. LAZAREVIĆ[b, *], M. RAJČIĆ-VUJASINOVIĆ[c], S. B. DIMITRIJEVIĆ[d], M. PETROVIĆ[b], M. GILIĆ[b], B. M. JOKIĆ[e]
[a]*Innovation Center Faculty of Technology and Metallurgy, University of Belgrade, Belgrade, Serbia*
[b]*Institute of Physics, University of Belgrade, P.O. Box 68, Belgrade, Serbia*
[c]*Technical Faculty in Bor, University of Belgrade, Bor, Serbia*
[d]*Mining and Metallurgy Institute Bor, Bor, Serbia*
[e]*Faculty of Technology and Metallurgy, University of Belgrade, Belgrade, Serbia*

The objective of this study was characterization of anodic film obtained when $Ag_{43}Cu_{37}Zn_{20}$ alloy was treated electrochemically in 3.5% wt. NaCl under potentiostatic conditions. At the potential of +0.25 V a complex multilayer film is formed. XRD shows that it consists of CuCl and zinc hydroxichlorides with a small amount of Cu_2O, probably formed in the film pores. The anodic film is a mixture of Cu_2O, CuCl, $Zn_5(OH)_8 \cdot H_2O$ and β-Zn(OH)Cl. Phases of the alloy, Ag and Cu rich, show different anodic behavior. It was assumed that all phonon lines in the obtained Raman spectra were of the Lorentzian type, which is one of the common type of lines for this kind of analysis. Phases of Ag, CuCl, β-Zn(OH)Cl, Cu_2O and $Zn_5(OH)_8(Cl)_2 \cdot H_2O$ were all registered by XRD.

(Received July 8, 2015; accepted September 29, 2016)

Keywords: $Ag_{43}Cu_{37}Zn_{20}$ alloy, Anodic film, Brazing materials, Raman spectroscopy

1. Introduction

Silver based brazing filler alloy are used for joining most ferrous and nonferrous metals, except Al and Mg. This classification includes a range of silver based filler metal compositions which may have various additions such as Cu, Zn, Cd, Sn, Mg, Ni and Li.

Generally speaking, the addition of Zn lowers the melting temperature of the Ag-Cu binary alloys and helps wet Fe, Co and Ni. Cd is also effective in lowering the brazing temperature of these alloys and assists in wetting a variety of base metals. Especially, Cd and Zn are vaporized during brazing.

The joining technique of copper alloy to steel has been widely applied in nuclear, aerospace and industry fields [1-3]. The conventional fusion welding of these materials usually leads to the irregularity interface and welding deficiency between copper alloy and steel [4, 5].

Silver based brazing filler alloys are commercially available as both wrought and cast products, including wire and cable, sheet, strip, plate, rod, bar, tubing, forgings, extrusions, castings and powder metallurgy shapes. Certain mill products, chiefly wire, cable and most tubular products, are used by customers without further metal working. On the other hand, most flat rolled products, rod, bar, mechanical wire, forgings and castings go through multiple metal working, machining, finishing and/or assembly operations before emerging as finished products.

Electrochemical properties in chloride solutions of the alloys that belong to the Ag-Zn-Cu system are investigated recently [6, 7]. These alloys do not show an anodic passive film region on polarization curves, although they have anodic film on the surface. The aim of the present work was to structural and spectroscopic study of electrochemically treated Ag-Cu-Zn alloy in 3.5% wt. NaCl.

2. Experimental procedures

The silver (99.99%), copper (99.99%) and zinc (99.995%) for electrode preparation were produced by recycling process. More details of the process and analytics can be found elsewhere [8-10]. The alloy for the electrode was prepared by ingot metallurgy method in two phases. The second, repeated, process was required due to high zinc losses for small charges. The obtained ingot was machined into cylinders with 7.14 mm diameter. It was subjected to homogenization annealing at 600 °C (T=0.92 Tmelt.) for 24 h in nitrogen atmosphere and slowly cooled for the next 8 h to the room temperature in the same protective atmosphere. Finally, the specimen was mounted in polytetrafluoroethylene mould. Chemical composition (wt.%) of the alloy used in the present study was 43.5% Ag, 37.7% Cu, 18.8% Zn, and trace amounts (in total less than 20 wt. ppm) of Pb, Sn, Ni, Fe and Cd, according chemical analysis performed by inductively coupled plasma atomic emission spectroscopy. This composition fulfills requirements of BS1845:1984 Ag5 standard [11].

All chemicals were of analytical grade produced by Merck (Germany). All solutions were prepared with ultra-

pure water of resistivity not less than 18 MΩ·cm. Test solution, 3.5 wt. % NaCl, was prepared by dissolving 35.000 g of NaCl in 1000 ml glass flask to the total mass of solution of 1000.00 g. pH value was adjusted to pH = 6.70 ± 0.15 by dropwise addition of 0.1 M NaOH solution.

X-ray Powder Diffraction (XRPD) patterns of investigated sample were obtained on a Philips PW-1050 diffractometer, operated at 40 kV and 30 mA, using Ni-filtered $CuK_{\alpha 1,2}$ radiation. The Bragg-Brentano focusing geometry was used with a fixed 1° divergence and 0.1° receiving slits. The patterns were taken in 10-100° 2θ range with step of 0.05° and exposure time of 6 s per step. For X-ray structural phase analysis, software EVA 9.0 Release 2003, Bruker AXS GmbH, Karlsruhe, Germany, was used.

The micro-Raman spectra were taken in the backscattering configuration and analyzed using a JobinYvon T64000 spectrometer, equipped with a nitrogen cooled charge-coupled-device detector. As an excitation source we used the 532 nm line of a Ti:sapphire laser. The measurements were performed at 20 mW laser power.

The alloy surface and corrosion products were studied using the scanning electron microscope (SEM model: JOEL JSM-6610LV operated at 20 kV) and field emission scanning electron microscopy (FEG-SEM model: TESCAN MIRA3 operated at 20 kV). Chemical composition of the alloy surface and products on surface were determined using energy dispersive X-ray spectroscopy (EDS). EDS detector was Oxford Instruments model X-Max SDD.

3. Results and discussion

Fig. 1 shows the results of X-ray diffraction (XRD) of the specimen after the potentiostatic test. The peaks of phases, ($Ag_{1-x-y}Cu_yZn_x$) solid solution and Cu_3Zn (α-brass) are present, as well as before the potentiostatic test.

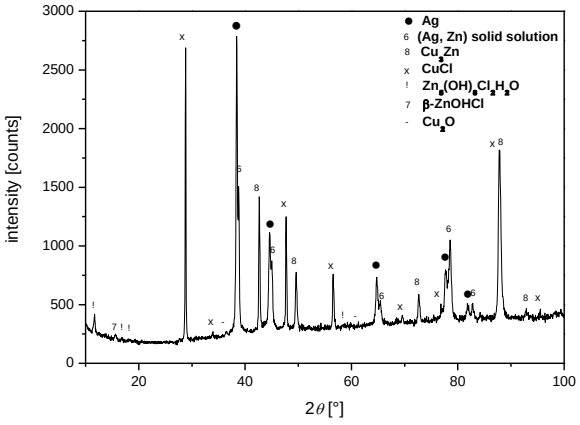

Fig. 1. RD pattern of the $Ag_{43}Cu_{37}Zn_{20}$ electrode after anodic potentiostatic polarization treatment at +0.25 V for 5 min in 3.5% wt. NaCl solution at 25 °C.

X-ray structural phase analysis was applied for identification the new phases formed after potentiostatic test using the EVA 9.0 computing program. It can be noticed that beside the peaks that belong to ($Ag_{1-x-y}Cu_yZn_x$) solid solution phase, the peaks that correspond to pure Ag phase also have appeared. They have been formed by reduction of Zn and Cu content in solid solution during the potentiostatic polarization at +250 mV. The peaks of ($Ag_{1-x-y}Cu_yZn_x$) solid solution phase are positioned at somewhat larger 2theta (2θ) values than the peaks of pure Ag phase. This difference increases with an increase of 2θ angles, meaning that the lattice parameter of Ag-rich phase is smaller than the lattice parameter of pure Ag phase, which can be explained by larger ionic radius of Ag than ionic radii of Zn and Cu. Noticeable increase of relative ratio of ($Ag_{1-x-y}Cu_yZn_x$) solid solution and pure Ag phases with the increase of 2θ angle implies that electrode surface is covered by pure Ag in thin layer beneath which is ($Ag_{1-x-y}Cu_yZn_x$) solid solution phase.

Fig. 2 shows the Raman spectra of the $Ag_{43}Cu_{37}Zn_{20}$ alloy recorded after anodic potentiostatic polarization treatment at +0.25 V for 5 min in 3.5% wt. NaCl solution at room temperature. The main Raman peaks are indicated in the spectrum. The presence of silver (Ag), cuprous chloride (CuCl), zinc hydroxychloride (β-Zn(OH)Cl), cuprous oxide (Cu_2O) and simonkolleite ($Zn_5(OH)_8(Cl)_2 \cdot H_2O$) is registered.

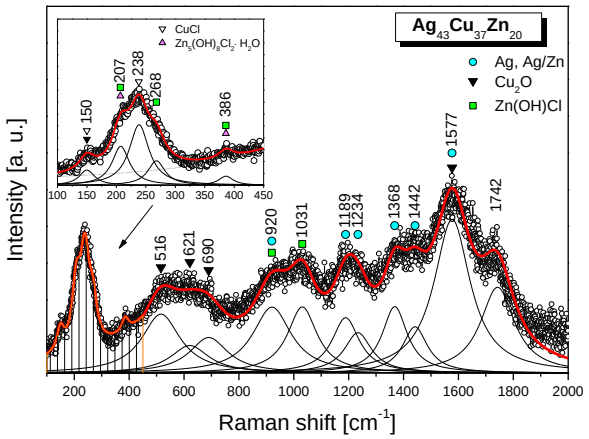

Fig. 2. Raman spectra of the $Ag_{43}Cu_{37}Zn_{20}$ alloy at room temperature.

Very strong silver peaks (cyan circles) indicate the formation of Ag areas, segregate from the Cu-Zn alloy. Observed Ag peaks at 920, 1189, 1234, 1368, 1442 and 1577 cm^{-1} are in general agreement with the previously published results [12].

Cuprous chloride has the cubic zinc blende structure with two atoms in the primitive cell so that there is only one triply degenerate fundamental optic mode, which is both Raman and infrared active. The first-order phonons of CuCl visible in Raman spectra (open triangles) are *TO*-phonon at 150 cm^{-1} and *LO*-phonon at 238 cm^{-1} [13, 14]. β-Zn(OH)Cl (green squares) are illustrated in Fig. 2. Three main peaks are observed at 207 and 268 cm^{-1}, assigned to a Zn-Cl bond, and 386 cm^{-1}, attributed to a Zn-O vibration

characteristic of this structure. Zinc hydroxychloride is also characterized by two main OH fundamental stretching bands at 920 and 1031 cm^{-1} [15, 16].

Cu_2O crystallizes in a cubic lattice with two molecules per unit cell and space group Pn3m. Since it exhibits inversion symmetry, its electronic and vibrational states are of definite parity. In the Raman spectra of treated alloy are seen several Cu_2O modes (black triangles). A weak mode at about 150 cm^{-1} can be a combination of *TO*-mode of CuCl and mode of Cu_2O. At 515, 621 and 690 cm^{-1} are modes of Cu_2O [17-19]. The Raman peaks at 207 and 386 cm^{-1} indexed by pink triangle, which agree very well with what are found in the [12], were assigned to $Zn_5(OH)_8(Cl)_2 \cdot H_2O$ (simonkolleite). A peak at 207 cm^{-1} was attributed to the Zn-Cl bond and that at 386 cm^{-1} to Zn-O which had a vibration characteristic of a simonkolleite structure. The presence of Ag, CuCl, β-Zn(OH)Cl, Cu_2O and $Zn_5(OH)_8(Cl)_2 \cdot H_2O$ is in agreement with the XRD results.

Fig. 3 shows a typical SEM image of surface film formed under potentiostatic condition over the Cu_3Zn phase. Two characteristics formations are observed, dark and bright features. At the level of surface of 100-200 pm^2 relatively homogeneously distributed crystals on the film surface are evident. Among the numerous crystals of irregular shape, those with tetrahedral structure are particularly recognized. CuCl has this structure although octahedral Cu_2O and hexagonal ZnO could have similar appearance. Dark parts of the image are micropores in the film structure. Position of the *fcc* structured crystals suggests chemical origin of the deposition. It is a characteristic of CuCl surface films on pure copper and brass. Fig. 3 indicates rapid crystal nucleation.

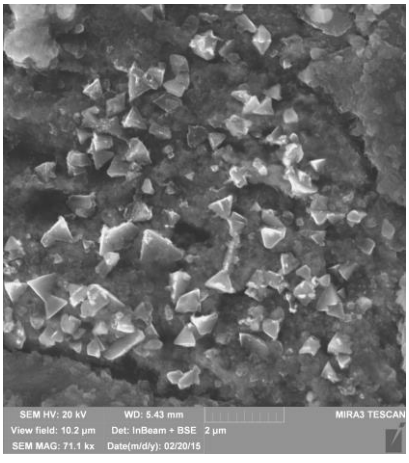

Fig. 3. FE SEM micrograph of the $Ag_{43}Cu_{37}Zn_{20}$ *alloy sample after potentiostatic polarization at +250 mV and for 300 s, part of surface film over* Cu_3Zn *phase*

These crevices are deep and could directly connect electrode surface and electrolyte. Crystals of CuCl smaller than 1 μm in different phases of formation and sizes in the range of magnitude order, from a few tens up to few hundreds of nm. Rounded grains are probably redeposited copper and black basic matrix is mixture of copper and zinc compounds revealed by XRD and Raman. This indicates that darker surfaces of anodic film originated from Cu_3Zn phase. It is possible that insoluble compounds of Cu and Zn originated form Ag solid solution as well, but since lower concentrations of soluble Cu (copper chloride complexes like $CuCl_2^-$ and $CuCl_3^{2-}$) it is unlikely that activity of these ions in the outer Helmholz plane exceeds the solubility equilibrium for the reaction: $CuCl_2^- \leftrightarrow CuCl_{(film)} + Cl^-$ [20]. Similar is for Zn soluble chloride complexes $ZnCl_4^{2-}$ and $Zn(OH)_2Cl_2^{2-}$ in relation with Zn(OH)Cl [21].

Very different surface is observed in the areas of over the silver solid solution (Fig. 4). These parts are formed over Ag-rich phase. Nanosized white grains are the main part of structure with some micro sized irregular shaped agglomerated particles. Basic structure (without agglomerates) is probably result of dealloying (mainly dezincation but also decopperization) of the Ag-rich phase as suggested from XRD analysis. SEM micrograph (Fig. 4) indicates that the structure is even more porous than the previous one shown in Fig. 3.

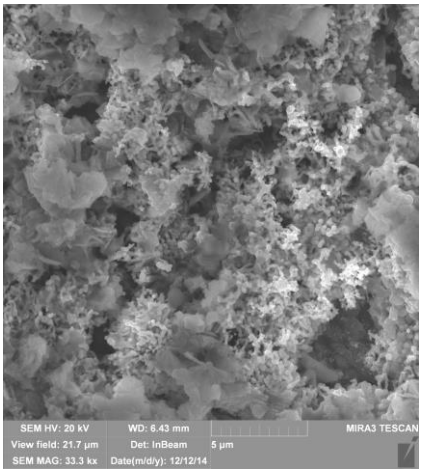

Fig. 4. FE SEM micrograph of the $Ag_{43}Cu_{37}Zn_{20}$ *alloy sample after potentiostatic polarization at +250 mV for 300 s, part of surface film over (Ag, Zn) solid solution.*

The compositions of areas shown in Fig. 3 and Fig 4, were determined by means of EDS. Absence of silver is characteristics of area in Fig. 3 and low concentration of Cu and Zn of area in Fig. 4. Lower concentration of Zn indicates dealloying of silver solid solution.

Table 1. EDS analysis in Fig. 3 and Fig 4.

Element/	O		Cl		Cu		Zn		Ag	
Area	At. %	Wt. %	At. %	Wt. %	At. %	Wt. %	At. %	Wt. %	At. %	Wt. %
Fig. 3	16.86	5.55	25.45	18.57	47.27	61.82	10.38	13.97	0.04	0.09
Fig. 4	21.51	4.70	9.11	4.41	15.98	13.87	2.82	2.52	50.58	74.50

4. Conclusions

The anodic film formed on alloy in 3.5% NaCl solution under potentiostatic conditions is a mixture of Cu_2O, CuCl, $Zn_5(OH)_8 \cdot H_2O$ and β-Zn(OH)Cl. Phases of the alloy, Ag and Cu rich, show different anodic behavior. For analysis of the Raman spectra it was assumed that all phonon lines were of the Lorentzian type, which is one of the common type of lines for this kind of analysis. That analysis combined with the XRD proved that phases of Ag, CuCl, β-Zn(OH)Cl, Cu_2O and $Zn_5(OH)_8(Cl)_2 \cdot H_2O$ form the anodic product on the electrode surface. Porosity of film at surface is confirmed by SEM images.

Acknowledgements

This research was financially supported by the Ministry of Education, Science and Technological Development of the Republic of Serbia through Projects No. III45003 and TR34033.

References

[1] A. F. Rowcliffe, S. J. Zinkle, J. F. Stubbins, D. J. Edwards, D. J. Alexander, J. Nucl. Mater. **258-263**, 183 (1998).
[2] K. Ioki, F. Elioa, V. Barabash, V. Chuyanov, V. Rozov, X. Wang, J. Chen, L. Wang, P. Lorenzetto, A. Peacock, M. Enoeda, H. Nishi, B. G. Hong, Y. H. Jeong, A. Gervash, I. Mazul, T. Tanaka, M. Ulrickson, Fusion Eng. Des. **82**, 1774 (2007).
[3] G. Le Marois, C. Dellis, J. M. Gentzbittel, F. Moret, J. Nucl. Mater. **233-237**, 927 (1996).
[4] H. Wang, K. Wang, R. Zheng, K. S. Prasad, S. P. Ringer, Mater. Charact. **59,** 542 (2008).
[5] I. Magnabosco, P. Ferro, F. Bonollo, L. Arnberg, Mater. Sci. Eng. A **424**, 163 (2006).
[6] A. Ntasi, Y. Al Jabbari, W. D. Mueller, G. Eliades, S. Zinelis, Angle Orthod. **84**, 508 (2014).
[7] S. P. Dimitrijević, M. Rajčić-Vujasinović, Ž. Kamberović, S. B. Dimitrijević, V. Grekulović, B. Trumić, A. Ivanović, Materials Transactions **56**, 2088 (2015).
[8] S. P. Dimitrijević, Z. Anđić, Ž. Kamberović, S. B. Dimitrijević, N. S. Vuković, Bulg. Chem. Commun. **46**, 814 (2014).
[9] A. Ivanović, S. Dimitrijević, S. Dimitrijević, B. Trumić, V. Marjanović, J. Petrović, N. Vuković, Optoelectron. Adv. Mat. **6,** 465 (2012).
[10] Z. Stanojević-Šimšić, S. Dragulović, S. Dimitrijević, V. Trujić, V. Conić, A. Ivanović, V. Gardić, Optoelectron. Adv. Mat. **6,** 1197 (2012).
[11] A. C. Davies, The science and practice of welding, **2**, The practice of welding, Cambridge University Press, Cambridge, United Kingdom (1993).
[12] H. Liang, Z. Li, W. Wang, Y. Wu, H. Xu, Adv. Mater. **21**, 4614 (2009).
[13] K. Fukushi, M. Nippus, R. Claus, Phys. Stat. Sol. (b) **86**, 257 (1978).
[14] S. Iwasa, E. Burstein, J. Physique **26**, 614 (1965).
[15] M. C. Bernard, A. Hugot-Le Goff, D. Massinon, N. Phillips, Corros. Sci. **35**, 1339 (1993).
[16] H. D. Lutz, M. Schmidt, B. Weckler, J. Raman Spectrosc. **24**, 797 (1993).
[17] A. L. Ma, S. L. Jiang, Y. G. Zheng, W. Ke, Corros. Sci. **91,** 245 (2015).
[18] A. Compaan, H. Z. Cummins, Phys. Rev. Lett. **31**, 41 (1973).
[19] R. J. Eliot, Phys. Rev. **124**, 340 (1961).
[20] D. Tromans, R. Sun, J. Electrochem. Soc. **138**, 3235 (1991).
[21] T. Kosec, I. Milošev, B. Pihlar, Appl. Sur. Sci. **253**, 8863 (2007).

*Corresponding author: lzorica@yahoo.com